JTCM Journal of Traditional Chinese Medicine

Online Submissions: http://www.journaltcm.com
ISSN 0255-2922
info@journaltcm.com

Original Article

Effect of Naoluoxintong formula (脑络欣通方) and its split prescriptions on cerebral vascular regeneration in rats with the cerebral ischemia-reperfusion

SHI Xiao, WANG Lina, HU Jianpeng, ZHANG Limiao, WANG Jin

SHI Xiao, HU Jianpeng, ZHANG Limiao, WANG Jin, Graduate School, Anhui University of Chinese Medicine, Hefei 230012, China
WANG Lina, Key Laboratory of Xin'an Medicine, Ministry of Education, Anhui University of Chinese Medicine, Hefei 230012, China
Supported by Second Round Construction Project of state administration of Traditional Chinese Medicine Academic School Inheritance Studio [Letter of Human Teaching (2019) No. 62 from State Administration of Traditional Chinese Medicine], the 13th Batch of "Innovation Team for Prevention and Treatment of Encephalopathy by Combination of Acupuncture and Medicine" Project of 115 Industry Innovation Team in Anhui Province [Anhui Talent Office (2020) No. 4] and Anhui Provincial Natural Science Foundation of China, studied the effects of Yiqi Huoxue Tongluo Method on Vascular Regeneration in Rats with Cerebral Ischemia and its Mechanism Based on Hypoxia-Inducible Factor 1A/Vascular Endothelial Growth Factor Signaling Pathway (KJ2022A0547)
Correspondence to: Prof. HU Jianpeng, Department of Graduate school, Anhui University of Chinese Medicine, Hefei 230012, China.
hujianpeng351@126.com
Telephone: +86-13739292867
DOI: 10.19852/j.cnki.jtcm.20221230.001
Received: June 11, 2022
Accepted: September 27, 2022
Available online: December 30, 2022

Abstract

OBJECTIVE: To observe regulatory effect of Naoluoxintong formula (脑络欣通方, NLXT) and its split prescriptions on vascular regeneration of rats suffering from cerebral ischemia-reperfusion (IR) syndrome of Qi deficiency with blood stasis (QDBS).

METHODS: NLXT is the representative prescription of Yiqi Huoxue Tongluo decoction (益气活血通络方), and NLXT is divided into Yiqi herbs (益气药) and Huoxue Tongluo herbs (活血通络药) according to their efficacies. One hundred and eight specific-pathogen-free, clean-grade, Sprague–Dawley male rats were selected to prepare the classical rat model with QDBS due to middle artery ischemia-reperfusion using the multi-factor compound simulation approach. The animals were classified into sham operation (S), model (M), Nimodping (NMDP), NLXT, YQ and HXTL groups, each having 18 rats. Cerebral ischemia was reperfused after 2 h, and 24 h later, they were administered traditional Chinese medicine treatment for 14 d twice a day. Angiogenesis changes after NLXT administration to middle cerebral artery occlusion-reperfusion (MCAO/R) rats with QDBS were analyzed using the neurological deficit score and hematoxylin-eosin staining. Cerebral infarct area by 2,3,5-Triphenyltetrazolium chloride was detected, and the ultrastructure of the blood vessel in the ischemic frontoparietal cortex was observed by transmission electron microscopy. Angiopoietin 1 (Ang1), angiopoietin 2 (Ang2), vascular endothelial growth factor A (VEGFA), vascular endothelial growth factor receptor 2 (VEGFR2), platelet endothelial cell adhesion molecule-1 (CD31), angiopoietin receptor 2 (Tie2), and P38 mitogen-activated protein kinase (MAPK) protein levels in the frontal and parietal cortex were quantified by immunofluorescence, reverse transcription-polymerase chain reaction, and Western blotting assays.

RESULTS: Relative to the S group, VEGFA and VEGFR2 levels in the frontal and parietal cortex of group M were increased, and Ang1, Ang2, Tie2, CD31, and p38 MAPK levels remarkably increased ($P < 0.05$); cerebral infarct area was significant and pathological morphology and ultrastructure damage was obvious. Relative to the group M, VEGFA, VEGFR2, CD31, Ang1, Ang2, and Tie2 expression of group NLXT and NMDP remarkably elevated ($P < 0.05$) and infarct focus, pathological morphology and ultrastructure were significantly improved; VEGFA and VEGFR2 levels in the groups YQ and HXTL increased, and Ang1, Ang2, CD31, and Tie2 levels remarkably increased ($P < 0.05$); p38 MAPK levels in the three treatment groups decreased ($P < 0.05$). Relative to the group NLXT, the expression levels of p38 MAPK in group YQ and group HXTL were significantly increased, and the expression levels of other indicators were significantly decreased ($P < 0.05$).

CONCLUSION: NLXT can promote the angiogenesis of the rat model of MCAO/R with QDBS by activating VEGFA and inhibiting P38 MAPK, and the effect is better than that of split prescription groups.

© 2023 JTCM. All rights reserved.

Keywords: infarction, middle cerebral artery; reperfusion; decomposed recipes; angiogenesis; Naoluoxintong

1. INTRODUCTION

Ischemic stroke is a disease with complicated etiology and pathogenesis. Owing to the high incidence of moderate to severe sequelae associated with it, the disease imposes great burdens on society and families and has become a major disease threatening the quality of human life and health.[1] Fibrinolysis and vascular regeneration after stroke are widely-studied areas, but hemorrhagic transformation and re-blockage caused by thrombolysis should be researched.[2] Middle cerebral artery ischemia is mainly caused by vascular obstruction and cerebral ischemia. Therefore, the timely establishment of lateral circulation during the window period of stroke occurrence and improvement of cerebral ischemia are extremely important for post-stroke repair. Vascular endothelial growth factor A (VEGFA) belongs to the platelet-derived growth factor (PDGF)/VEGF growth factor family, enhancing angiogenesis. VEGF is a factor that specifically promotes vascular endothelial mitosis, regulates angiogenesis, and can induce angiogenesis alone.[3-6] VEGFA can activate and downregulate the expression of Ang1, Ang2, and its receptor Tie2 to exert angiogenic effect by binding to its receptor VEGFR2.[7] CD31 is expressed in high density on the outer edge of vascular endothelial cells.[8,9] P38 mitogen-activated protein kinase (MAPK) is related to the ischemic stroke pathogenic mechanism.[10] As reported by Liu Bei *et al*,[11] inhibiting the P38 MAPK signaling pathway results in neurovascular regeneration and neuroprotection which helped to treat different nervous system disorders. “Naoluoxintong formula (脑络欣通方, NLXT)”, originated from the internal medicine department of Wang Family of Xin'an, is based on the *Qi* and blood theory, with Yiqi Huoxue Tongluo decoction (益气活血通络方) as the representative prescription of treatment, and has efficacy in the long-term clinical practice.[12] Previous studies have reported that NLXT can participate in the angiogenesis of ischemic stroke by activating VEGF,[13] but the drug action mechanism has not been elucidated, and further exploration is required. In the present study, based on the results of previous studies and using NLXT and its split prescriptions as the breakthrough point, the classical rat model with *Qi* deficiency and blood stasis (QDBS) caused by middle cerebral artery occlusion-reperfusion was used, and the different intervention of Traditional Chinese Medicine (TCM) therapy and medicines was used to investigate the drug action mechanisms of YQHXTL therapy on cerebrovascular regeneration in rats.

2. MATERIALS AND METHODS

2.1. Animals and ethical approval

Male specific pathogen free Sprague-Dawley rats of clean grade (240-280 g) were obtained from Pizhou Dongfang Culture Corp. Ltd. [certificate No. SCXK (SU) 2017-0003; animal ethics approval number: AHUCM-rats-2021019]. Later, the animals were raised within the animal facility of Ministry-of-Education Key Laboratory at Xin’an Medicine, the Anhui University of Chinese Medicine under (22 ±1) ℃, 60% relative humidity, and 12 h/12 h light/dark cycles, and were allowed to drink water and eat fodder freely. In line with the digital random approach, we classified animals into sham operation, model, Nimodping, NLXT, YQ and HXTL groups, each having 18 rats. The experiment was conducted after adaptive feeding for a week. All experiments were approved by the Committee on the Ethics of Animal Experiments of the Anhui University of Chinese Medicine.

2.2. Preparation and administration method of TCM

The herbs of NLXT consist of Huangqi (*Radix Astragali Mongolici*, 30 g, lot: 2105160132), Sanqi (*Radix Notoginseng*, 10 g, lot: 2108110026), Chuanxiong (*Rhizoma Chuanxiong*, 6 g, lot: 2106080158), Tianma (*Rhizoma Gastrodiae*, 10 g, lot:2108160163), Honghua (*Flos Carthami*, 10 g, lot: 21120903), Danggui (*Radix Angelicae Sinensis*, 10 g, lot: 2111240115), and Wugong (*Scolopendra*, 4 g, lot: 21072206). YQ herbs consist of Huangqi (*Radix Astragali Mongolici,* 30 g) as a single ingredient. HXTL herbs consist of Sanqi (*Radix Notoginseng,* 10 g), Chuanxiong (*Rhizoma Chuanxiong,* 6 g), Tianma (*Rhizoma Gastrodiae,* 10 g), Honghua (*Flos Carthami,* 10 g), Danggui (*Radix Angelicae Sinensis,* 10 g), and Wugong (*Scolopendra,* 4 g). They were provided by First Hospital Affiliated to the Anhui University of Chinese Medicine and prepared into liquid medicine. NMDP (Yabao Pharmaceutical Group Co., Ltd., national drug approval number: H14022821). According to Pharmacological Experimental Methodology,[14] the medium dose of Chinese herbal compound was taken from adults and converted according to the conversion coefficient of body surface area between human and rats, those model rats were intragastrically administered with 7.2, 2.7, 4.5 g/kg and 8.1 mg/kg, for 14 d, twice a day, on the second day of replication of the MCAO/R model with QDBS syndrome, whereas other groups were intragastrically administered with the same amount of normal saline.

2.3. Reagents and instruments

The VEGF-A polyclonal antibody (art. No. ABP56497) and VEGFR-2 polyclonal antibody (Art. No. ABP55018) were purchased from Wuhan Abbkine Company (Wuhan, China). The CD31 antibody (Art. No. 1002284) was obtained from Novus Biologicals (Littleton, CO, USA). The Tie2 antibody (batch number: AI11187724) was purchased from Beijing Bioss Biotechnology Company (Beijing, China). The anti-p38 alpha/MAPK14 antibody (batch number: GR3215674-1) was obtained from Shanghai Abcam Company (Shanghai, China). Fluorescein isothiocyanate (FITC)-labeled goat anti-

rabbit immunoglobulin G (IgG) (batch number: 202700514) was obtained from Beyotime Biotechnology (Shenzhen, China). Osmic Acid (batch number: 18456) was obtained from Ted Pella Inc (Aldina, CA, USA). The reverse transcription-polymerase chain reaction test kit (batch number: AKF1919A) was provided by TaKaRa Biotechnology (Dalian, China). Sangon Biotech Company synthesized the primers (Shanghai, China). Automatic Embedding Machine (model: EG1150H) and Closed Microtome (model: 2135) were purchased from Leica (Heidelberg, BadenWuerttemberg, Germany). PowerPac Basic Electrophoresis Apparatus (model: EPS300) was purchased from Bio-Rad (Shanghai, China). Electrophoresis Tank (model: VE-180) and Transmembrane Apparatus (model: VE-186) were purchased from Tanon (Shanghai, China). Chemiluminescence Imaging System (model: FluorChem FC3) was purchased from ProteinSimple (Silicon Valley, CA, USA). High-Efficiency Fluorescence Microscope (model: BX51) and Digital Camera (model: DP70) were purchased from Olympus (Beijing, China). Electron transmission electron microscope (model: JEM1400) were purchased from JEOL Ltd. (Zhaodao, Japan).

2.4. Surgery procedures of MCAO/R

The animal model of QDBS syndrome was reproduced by the multi-factor compound method by Tanhui *et al*.[15] (a) Starvation: the experimental rats were fed with 40 g/kg diet twice a day, 2/3 of the whole day's dose in the morning, and the remaining 1/3 in the evening. (b) Fatigue: the experimental rats were kept in a bucket in 5 batches, with the water temperature and room temperature maintained at (10 ± 2) ℃, and forced to swim until fatigued by dialing with a wooden stick. (c) Cold dampness: rats were exposed to the air in a closed room for natural drying. (d) Panic: unwatered rats were kept aside to watch and listen to the struggling sound when rats were swimming. (e) High-fat diet: 5 mL/kg fat milk was added to the daily diet of experimental rats. After 10 d, the preparation of MCAO/R animal models was started. First, each rat was given anesthesia through intraperitoneal injection of 3% pentobarbital (30 mg/kg). Later, their head and limbs were fixed onto the rat plate on their back. The operation site was exposed and disinfected, followed by passive separation of the right common carotid artery, external/internal carotid arteries (ECA/ICA), and electrocoagulation of the superior thyroid artery and pterygopalatine artery. The external carotid artery was cut off from the two ligations, a V-shaped incision was cut from the near free terminal of ECA, whereas a fishing line was inserted into the ICA about 18 mm.[15,16] At 2 h later, we slowly pulled the fishing line out for about 5 mm; thus, causing ischemia-reperfusion injury. Only artery dissection was performed in the sham operation group.

According to Longa *et al*,[16] scoring and quantitative standards of the model biological characteristics[15] were considered. Successful standard of MCAO/R model of QDBS syndrome: (a) neurological deficit score: 2-3 points (Table 1); (b) the scores of *Qi* deficiency syndrome and blood stasis syndrome are 10-20 points (Tables 2 and 3). According to the standard of the neurological deficit scores and the QDBS syndrome scores, the total success rate of modeling and the total mortality rate were 93.52% and 5.56%, respectively. Given the impact of these factors on sample size, so the actual number of rats purchased, raised and modeled was greater than the planned number. The model numbers have been supplemented in time, so the experimental results are not significantly affected. The modeling success and mortality rates of each group are shown in the following Table 4.

Table 1 Zea-longa (0-4 points) scoring criteria

Neurological deficit	Score (points)
No neurological impairment	0
cannot extend the contralateral forepaw	1
Turn outward	2
Dump to the opposite side	3
Inability to walk spontaneously,	4

2.5. Brain tissue sampling

The rats were intraperitoneally injected with 3% pentobarbital (30 mg/kg) for anesthesia the next day after gavage. Following 14 d of cerebral ischemia-reperfusion treatment, we selected six rats from every group and obliquely fixed the anesthetized rats on the rat board. A small opening cut was performed in the right atrial appendage. Afterward, we kept a blunt catheter from the left ventricle to the aorta, and 200 mL of normal saline was rapidly injected until the liver became white. Then, paraformaldehyde was continuously injected until the rat tail was erect, the limbs were stiff, and the brain was

Table 2 Syndrome differentiation scale of *Qi* deficiency syndrome in rats

Qi deficiency symptom	
Mental fatigue, poor mobility; hair withered; no appetite, mild loose stool	3 points each
Lethargy; hair fringe; moderate loose stool	5 points each
Poor or absent antagonistic behavior; hair is sparse and easy to fall; severe loose stool with yellow-green smelly poop	7 points each

Table 3 Syndrome differentiation scale of blood stasis syndrome in rats

Blood stasis syndrome	
Bleak tongue; eyeball turns pale red; the color of rat tail is dim	3 points each
Purple tongue; eyeball turns dark red; mouse tail slightly purple with blood stasis	5 points each

Table 4 Table of success rate and death rate of models in each group (%)

Group	Model success rate	Mortality rate
S	100	0
M	88.89	11.11
NMDP	94.44	5.56
NLXT	94.44	5.56
YQ	94.44	5.56
HXTL	88.89	11.11

Notes: S: Sham group (saline, 14 d); M: Model group (saline, 14 d); NMDP: Nimodiping group (8.1 mg/kg, 14 d); NLXT: Naoluoxintong group (7.2 g/kg, 14 d); YQ: Yiqi group (2.7 g/kg, 14 d); HXTL: Huoxuetongluo group (4.5 mg/kg, 14 d).

taken out after decapitation. The brain was taken out after being stored for 1 week in a refrigerator at 4 ℃. The telencephalon was removed before the anterior optic chiasm, and a part of the brain tissue was removed. The upper and lower sections were parallel and then put into an embedding box for routine dehydration, transparency, embedding, and slicing. Then, we selected six anesthetized rats from every group, quickly decapitated them, the brain was taken out and kept on the ice, and the ischemic frontoparietal cortex was quickly separated on the ice and stored at −80 ℃ in a refrigerator.

2.6. Cerebral infarct area

The experimental rats were narcotized with 3% pentobarbital sodium, and the brain was taken out after quick decapitation. The water solution was removed by filter paper and the samples were frozen at −20 ℃ for 20 min. The coronal sections were cut into 2 mm thick slices, which were immersed in 2% 2, 3, 5-triphenyltetrazolium chloride solution and incubated at 37 ℃ for 20 min. The slices were taken out for sequencing and photographing. The infarct area was evaluated using imageJ software.

2.7. Hematoxylin-eosin staining

The wax block was sliced, dewaxed, debenzolized, stained with hematoxylin and eosin, dehydrated, made transparent, and dried with neutral gum. Histomorphological changes of the ischemic frontal-parietal cortex were observed using a microscope.

2.8. Immunofluorescence staining

After slicing, they were dried in a thermostatic oven, dewaxed, debenzenylated, washed with water, and subjected to antigen high-pressure repair, cooling, distilled-water washing, drew a hydrophobic circle around the tissue, rinsed by phosphate buffer solution (PBS) with Twin 20 (PBS-T), incubated using 0.5% TritonX-100 for 1 h at room temperature, incubated with goat serum blocking solution for 30 min under ambient temperature, followed by incubation using primary antibodies CD31 (1∶200), VEGFA (1∶200), and VEGFR2 (1∶300), respectively, and incubated overnight at the 4 ℃. Following washing by PBS-T, we added FITC-labeled goat anti-rabbit IgG (1∶400) dropwise, followed by 30-min sample incubation under ambient temperature in the dark and rinsing by PBS-T thrice. Each slide was sealed by anti-fluorescence quenching sealing tablets (including 4',6-diamidino-2-phenylindole) and photographs were taken using the fluorescence microscope.

2.9. Ultrastructure of cerebral microvessels

The cortical tissue was taken and cut into 1 mm × 1 mm ×1 mm tissue blocks, which were then quickly fixed with 2.5% glutaraldehyde (electron microscope-grade), rinsed, fixed with 1% hydrochloric acid, rinsed, gradient dehydrated with acetone, embedded with 812 resin, and ultrathin sectioned. The ultrastructure of blood vessels was observed under the transmission electron microscope.

2.10. Microvessel density

According to the Weidner[17] modified blood vessel counting method, we considered that a blood vessel with a diameter of < 6 red blood cells' diameter or a single cell positive at the same time and the boundary with the surrounding cells was a new blood vessel. The number of standard positive CD31-labeled vessels was counted at high power (× 400), and the results for each sample are expressed as an average number of vessels in 3 high-power fields.

2.11. Western blotting

About 0.1 g of the frontoparietal cortex of the brain was measured from the six frozen samples, homogenized, and lysed with 0.6 mL of radioimmunoprecipitation assay cell lysate (containing 0.6 mmol/L phenylmethylsulfonyl fluoride). It was then centrifuged at 12000 rpm and 4 ℃ for 15 min; supernatants containing total tissue protein were collected. Afterward, the proteins were separated by 10% sodium dodecyl sulfate polyacrylamide gel electrophoresis, then transferred on the polyvinylidene fluoride membranes. Then, membranes were blocked by 5% defatted milk, followed by overnight incubation with antibodies against Tie2 (1∶1000) and p38 MAPK (1∶2000) under 4 ℃. The samples were later rinsed, followed by 1.2 h incubation with horseradish peroxidase (1∶2000) under ambient temperature. We used an electro-chemiluminescence kit to detect proteins, and the Image J software was used for band collection and analysis.

2.12. Reverse transcription-polymerase chain reaction (RT-PCR)

Six frozen samples were taken, total cerebral cortical RNA was extracted by TRIzol reagent, followed by reverse transcription into cDNA. RT-PCR was performed with a fluorescent quantitative PCR machine, with β-actin being the endogenous control. Table 5 shows the sequences of all primers.

2.13. Statistical analysis

The data are represented as mean ± standard deviation ($\bar{x} \pm s$). SPSS 25.0 (IBM Corp., Armonk, NY, USA) software was adopted for statistical analysis. One-way analysis of variance (ANOVA) was performed for comparing different groups. Before ANOVA analysis, we adopted a normal distribution test to ensure the normality of the data. In addition, we used the least

significant difference approach to compare variance homogeneity between the groups, whereas Tamhane T2 approach was used to compare variance heterogeneity. $P < 0.05$ indicated statistical significance.

3. RESULTS

3.1. NLXT attenuated the neurological deficit scores and the QDBS syndrome scores of experimental rats more significantly than split prescription groups

The neurological deficit scores before and after treatment are summarized in Table 6. Relative to the S group, the M group showed markedly increased neurological deficit scores, *Qi* deficiency scores, and blood stasis scores ($P < 0.05$). Compared with the M group, the neurological deficit score, *Qi* deficiency score, and blood stasis score remarkably decreased ($P < 0.05$) in those four treatment groups, whereas the scores of the NLXT and NMDP groups were significantly reduced ($P < 0.05$).

3.2. NLXT reduces the area of cerebral infarction in the experimental rats more significantly than split prescription groups

Supplement Figure 1 shows TTC staining results. Compared with the S group (Table 7), the M group had a significant infarct size, and the infarct size was significantly larger than that in the normal group ($P < 0.01$). Compared with the M group, NMDP and NLXT groups could significantly reduce the cerebral infarction area in rats ($P < 0.01$).

3.3. NLXT attenuated pathological changes in ischemic side brain tissue of experimental rats more significantly than split prescription groups

Figure 1 shows HE staining results. S group showed normally arranged cells with clear outlines of the nuclei and cytoplasm. The cells were intact, and their morphology and structure were normal, such as cell membrane, cell nucleus, cytoplasm, and cell body are clear and distinct. Compared with the S group, the M group had loosely and disorderly arranged cells, and karyopycnosis, fragmentation, and hyperchromatism were evident in the model group. Compared with the M group, the NLXT and NMDP group had a relatively complete cell morphological structure, with the cells arranged neatly and all nuclei almost intact. In the YQ and HXTL groups, the morphological structure and arrangement of cells with mild cellular tissue damage were abnormal, such as cell arrangement disorder, nuclear shrinkage relative to the M group.

3.4. NLXT can improve the ultrastructure of brain tissue in the frontoparietal and parietal cortex of experimental rats more significantly than split prescription groups

In Group S, the microvessels were regular in shape, the

Table 5 Quantitative polymerase chain reaction primer sequence

Gene	Amplicon size (bp)	Forward (5'→3')	Reverse (5'→3')
β-actin	150	CCCATCTATGAGGGTTACGC	TTTAATGTCACGCACGATTTC
Ang–1	169	ATGCCAGATACTGCGAAAGT	GTGATCTGGAAGGGAGACTG
Ang-2	133	GAACTTGCTGCATCCAAAGAT	CTAAGTGATGTGCGTCAGTC

Table 6 Effect of Naoluoxintong and its split prescriptions on the neurological deficit score, *Qi* deficiency score, and blood stasis score of the experimental rats ($\bar{x} \pm s$)

Group	*n*	Neurological deficit score (points)	*Qi* deficiency score (points)	Blood stasis score (points)
S	18	0.0±0.0	3.4±1.2	3.8±1.4
M	18	2.6±0.5[a]	13.4±2.6[a]	13.8±2.5[a]
NMDP	18	0.4±0.5[b]	4.6±1.6[b]	5.2±2.4[b]
NLXT	18	0.6±0.5[b]	5.4±2.3[b]	6.4±2.1[b]
HXTL	18	1.7±0.7[bc]	10.1±1.8[bc]	11.1±2.2[bc]
YQ	18	1.7±0.6[bc]	10.3±1.6[bc]	11.2±2.0[bc]

Notes: S: Sham group (saline, 14 d); M: Model group (saline, 14 d); NMDP: Nimodiping group (8.1 mg/kg, 14 d); NLXT: Naoluoxintong group (7.2 g/kg, 14 d); YQ: Yiqi group (2.7 g/kg, 14 d); HXTL: Huoxuetongluo group (4.5 mg/kg, 14 d). [a]$P < 0.05$ *vs* S; [b]$P < 0.05$ *vs* M; [c]$P < 0.05$ *vs* NLXT.

Table 7 Effect of Naoluoxintong and its split prescriptions on the cerebral infarction area in the experimental rats ($\bar{x} \pm s$)

Group	*n*	Cerebral infarction area	VEGFA	VEGFR2	CD31
S	6	0.00±0.00	16.33±1.21	11.83±1.17	2.18±0.11
M	6	25.77±1.36[a]	18.50±1.38	15.5±1.05	5.83±0.30[a]
NMDP	6	12.38±1.10[b]	39.50±3.62[b]	37.17±2.32[b]	19.14±1.91[b]
NLXT	6	13.80±1.63[b]	39.17±2.79[b]	35.83±2.32[b]	19.63±0.44[b]
YQ	6	23.31±0.84[c]	21.50±1.87[b]	21.17±1.94[bc]	13.80±0.92[bc]
HXTL	6	21.45±1.60[bc]	23.17±1.48[bc]	23.17±1.47[bc]	11.95±0.43[bc]

Notes: S: Sham group (saline, 14 d); M: Model group (saline, 14 d); NMDP: Nimodiping group (8.1 mg/kg, 14 d); NLXT: Naoluoxintong group (7.2 g/kg, 14 d); YQ: Yiqi group (2.7 g/kg, 14 d); HXTL: Huoxuetongluo group (4.5 mg/kg, 14 d). VEGFA: vascular endothelial growth factor A; VEGFR2: vascular endothelial growth factor receptor 2; CD31: platelet endothelial cell adhesion molecule-1. [a]$P < 0.01$ *vs* S; [b]$P < 0.01$ *vs* M; [c]$P < 0.01$ *vs* NLXT.

endothelial cells were in good condition, the organelles were abundant, and the intercellular junction was tight. Compared with group S, the endothelial cells in group M were structurally loose, with mitochondria swelling, membrane rupture, most of the cristae dissolved, and the microvascular lumen compressed and occluded. Compared with group M, the double-layer membrane structure with tight intercellular junction of endothelial cells in YQ and HXTL groups gradually recovered, but mitochondrial swelling, membrane rupture, cristae dissolution, and vascular compression were not significantly improved; however, the microvascular lumens in NMDP and NLXT groups were normal, the double-layer membrane structure with tight intercellular junction in endothelial cells was clear, the number of mitochondria was increased, and the mitochondrial cristae were restored, basically close to the normal group (Figure 2).

3.5. NLXT increased VEGFA and VEGFR2 levels in the frontoparietal and parietal cortex of experimental rats more significantly than split prescription groups

The experimental results of immunofluorescence are presented in Figure 3 and Table 7. The differences in VEGFA and VEGFR2 levels were not significant in the M group versus the S group ($P > 0.05$). Relative to the M group, VEGFA and VEGFR2 expressions among the four treatment groups was different degrees of up-regulation; similarly, those indicators of NLXT and NMDP groups are remarkably increased ($P < 0.05$). The levels of VEGFA and VEGFR2 in the YQ and HXTL groups were significantly lower than those in the NLXT and NMDP groups ($P < 0.05$), but still higher than those in the S and M groups. However, there was no significant difference in the expression of VEGFA and VEGFR2 between NLXT and NMDP groups.

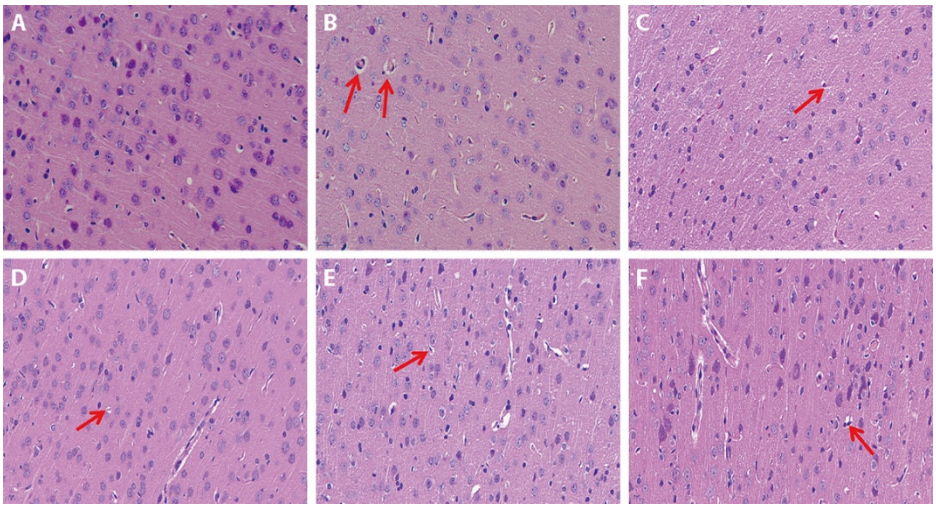

Figure 1 Effect of Naoluoxintong and its split prescriptions on the morphology of the cerebral cortex of ischemic frontal cortex in the experimental rats (hematoxylin and eosin staining, × 400, $n = 6$)
A-F: typical image showing pathological sections. A: Shame group (saline, 14 d); B: Model group (saline, 14 d); C: Nimodiping group (8.1 mg/kg, 14 d); D: Naoluoxintong group (7.2 g/kg, 14 d); E: Yiqi group (2.7 g/kg, 14 d); F: Huoxuetongluo group (4.5 mg/kg, 14 d). Red arrows show degenerated and necrotic nerve cells.

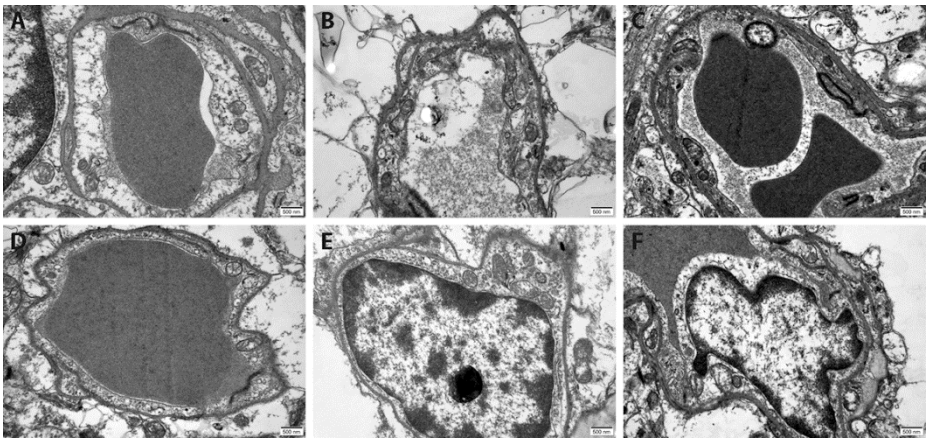

Figure 2 Effect of Naoluoxintong and its split prescriptions on the ultrastructure of blood vessels in ischemic frontal cortex of experimental rats (glutaraldehyde staining, × 25 000, $n = 6$)
A-F: typical image showing pathological sections. A: Shame group (saline, 14 d); B: Model group (saline, 14 d); C: Nimodiping group (8.1 mg/kg, 14 d); D: Naoluoxintong group (7.2 g/kg, 14 d); E: Yiqi group (2.7 g/kg, 14 d); F: Huoxuetongluo group (4.5 mg/kg, 14 d).

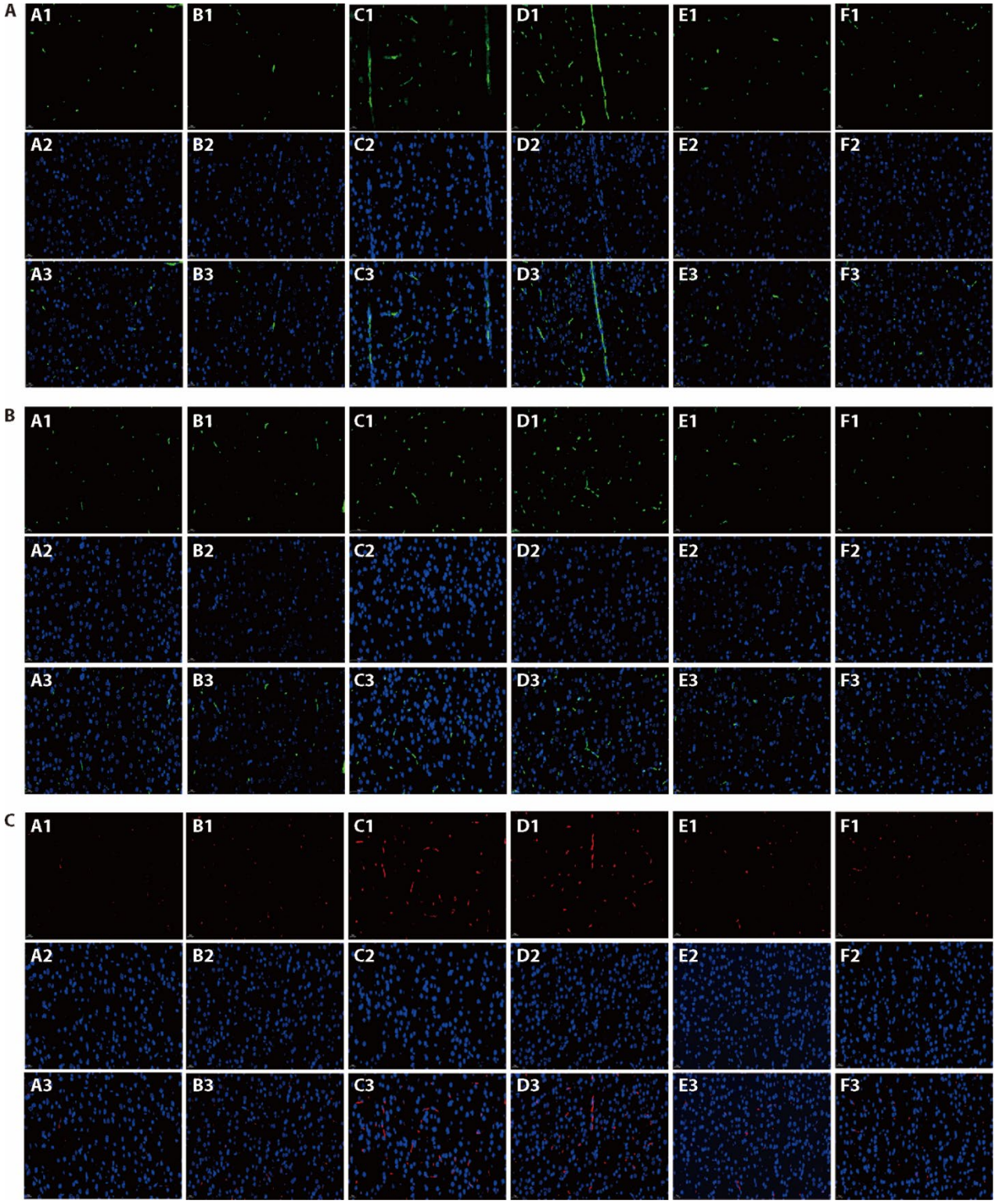

Figure 3 Effect of Naoluoxintong and its split prescriptions on the VEGFA, VEGFR2 and CD31 protein expression within frontoparietal cortex in the experimental rats (immunofluorescence staining, × 400, n = 6)

A/B/C: representative images of a histological section of VEGFA/ VEGFR2/CD31; A1, A2, and A3 are VEGFA/VEGFR2, DAPI, and Merge, respectively, in the sham group (saline, 14 d); B1, B2 and B3 were VEGFA/VEGFR2/CD31, DAPI, and Merge, respectively, in the model group (saline, 14 d); C1, C2 and C3 were VEGFA/VEGFR2/CD31, DAPI, and Merge, respectively, in the Nimodiping group (8.1 mg/kg, 14 d); D1, D2 and D3 were VEGFA/VEGFR2/CD31, DAPI, and Merge, respectively, in the Naoluoxintong group (7.2 g/kg, 14 d); E1, E2 and E3 were VEGFA/VEGFR2/CD31, DAPI, and Merge, respectively, in the Yiqi group (2.7 g/kg, 14 d). F1, F2 and F3 VEGFA/VEGFR2, DAPI, and Merge, respectively, in the Huoxuetongluo group (4.5 mg/kg, 14 d). VEGFA: vascular endothelial growth factor A; VEGFR2: vascular endothelial growth factor receptor 2; CD31: platelet endothelial cell adhesion molecule-1.

3.6. NLXT increased CD31-positive neovascularization in the frontal and parietal cortex of the experimental rats more significantly than split prescription groups

Microvascular counting results are presented in Figure 3 and Table 7. Relative to the S group, the M group had markedly increased CD31-positive neovascular density ($P < 0.05$); compared with the M group, the four treatment groups had markedly higher CD31-positive neovascularization density ($P < 0.05$); the expression of CD31-positive neovascularization level in the YQ and HXTL groups was significantly lower than that in the NLXT and NMDP groups ($P < 0.05$), but still higher than that in the S and M groups. The CD31-positive neovascularization level of NMDP group tended to increase compared to NLXT group, but the difference was not statistically significant.

3.7. NLXT increased the levels of Tie2 and attenuated p38 MAPK in the frontal and parietal cortex of rats more significantly than split prescription groups

The Western blotting results are presented in Figure 4 and Table 8. Relative to the S group, the M group had increased Tie2 and p38 MAPK protein levels ($P < 0.05$). Relative to the M group, Tie2 protein levels of the four treatment groups were remarkably upregulated ($P < 0.05$), and p38 MAPK protein levels in the four treatment groups drastically decreased ($P < 0.05$). Compared with the NLXT group, the expression level of Tie2 protein in the YQ and HXTL groups was obviously lower, but still higher than that in the S and M groups, whereas that of p38 MAPK protein increased in the YQ and HXTL groups, but still lower than M group ($P < 0.05$). However, there was no significant difference in the expression of Tie2 and p38MAPK between NLXT and NMDP groups.

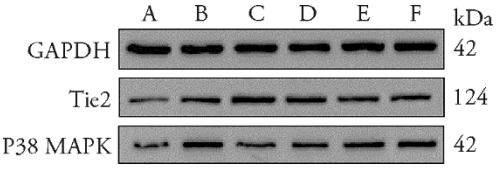

Figure 4 Effect of Naoluoxintong and its split prescriptions on the protein levels of Tie2 and p38 MAPK in the frontoparietal cortex of the experimental rats
A: Shame group (saline, 14 d); B: Model group (saline, 14 d); C: Nimodiping group (8.1 mg/kg, 14 d); D: Naoluoxintong group (7.2 g/kg, 14 d); E: Yiqi group (2.7 g/kg, 14 d); F: Huoxuetongluo group (4.5 mg/kg, 14 d). GAPDH: glyceraldehyde-3-phosphate dehydrogenase; Tie2: angiopoietin receptor 2; P38MAPK: P38 mitogen-activated protein kinase.

3.8. NLXT increased Ang1 and Ang2 levels in the parietal and frontal cortices of rats more significantly than split prescription groups

The results of RT-PCR are presented in Table 8. Compared with the S group, Ang1 and Ang2 protein levels of M group was remarkably elevated ($P < 0.01$). Relative to the M group, Ang1 and Ang2 protein levels in the four treatment groups were dramatically increased ($P < 0.01$). Compared with the NLXT group, the protein levels of Ang1 and Ang2 in the YQ and HXTL groups were markedly decreased ($P < 0.01$), but still higher than those in the S and M groups; however, the expression of Ang1 and Ang2 between the NMDP and NLXT groups were not statistically significant.

4. DISCUSSION

The focal cerebral ischemia-reperfusion injury in this study was a non-infectious inflammatory brain injury.[18] After ischemia, the ischemic endothelial cells begin to proliferate, induce vascular regeneration, and promote functional recovery.[19] Some studies have reported transient ischemia and the beginning of ischemic endothelial cell proliferation within 12-24 h.[20] Therefore, treating stroke with vascular regeneration and establishing collateral circulation are necessary.

VEGF is highly correlated with new blood vessel formation and promotes endothelial cell growth, invasion, and vessel formation. VEGF mRNA or VEGF protein is expressed in astrocytes and neurons on the ischemic side.[21,22] As the VEGF family member, VEGFA can bind to the receptor VEGFR2, which has a critical function during cerebrovascular regeneration.[23] VEGFA and Ang2 are angiogenic factors involved in angiogenesis,[24] and Tie2 is a receptor for Ang1 and Ang2. After the intervention with relevant anti-angiogenic drugs, the RT-PCR results indicated the downregulation of equal-angiogenesis-related mRNA expression, including VEGFA, VEGFR2, and Tie2, thereby inhibiting vascular endothelial cell migration.[25] Meanwhile, in angiogenesis studies, VEGFA, VEGFR2, Ang1, Ang2, and Tie2 levels were the same as the trend of CD31, which is a platelet-endothelial cell adhesion molecule participating in angiogenesis.[26,27] Studies have reported that the number of angiogenesis can be studied using CD31 markers to assess the mechanism and state of vascular regeneration.[28]

The integration of TCM with western medicine can facilitate neurological recovery from cerebral IR damage. TCM is widely applied in Asia to treat cerebral ischemia-reperfusion injury because of its multi-target uniqueness. The YQHXTL herbs are commonly used treatment options for cerebral ischemia-reperfusion.[29] In this study, the different efficacies of herbs on the vascular regeneration of rats with MCAO/R caused by QDBS syndrome were studied. We found that rats in the model group had obvious infarct focus, pathological and ultrastructural changes were obvious during the study, which indicated that the function was damaged after cerebral ischemia-reperfusion. After TCM intervention, when CD31, VEGFA, and VEGFR2 were further increased slowly in the YQ and HXTL groups, the levels of Ang1, Ang2, and Tie2 were significantly increased, whereas the five indicators contents of NLXT group remarkedly elevated and NLXT reduced the cerebral infarction area of ischemia-reperfusion and improved the histopathological morphology and ultrastructure

Table 8 Effect of Naoluoxintong and its split prescriptions on P38MAPK, Tie2, Ang1 and Ang2 protein levels in the frontoparietal cortex of the experimental rats ($\bar{x} \pm s$)

Group	*n*	p38MAPK	Tie2	Ang1	Ang2
S	6	0.290±0.084	0.220±0.081	1.004±0.103	1.010±0.146
M	6	0.913±0.118[a]	0.420±0.119[a]	1.322±0.131[a]	1.646±0.226[a]
NMDP	6	0.398±0.052[b]	0.839±0.134[b]	2.392±0.406[b]	3.692±0.691[b]
NLXT	6	0.450±0.016[b]	0.896±0.111[b]	2.226±0.220[b]	3.421±0.371[b]
YQ	6	0.727±0.080[bc]	0.675±0.068[bc]	1.569±0.072[bc]	2.151±0.216[bc]
HXTL	6	0.767±0.116[bc]	0.642±0.122[bc]	1.814±0.078[bc]	2.531±0.402[bc]

Notes: S: Sham (saline, 14 d); M: Model (saline, 14 d); NMDP: Nimodiping (8.1mg/kg, 14 d); NLXT: Naoluoxintong (7.2 g/kg, 14 d); YQ:Yiqi (2.7 g/kg, 14 d); HXTL: Huoxuetongluo (4.5 mg/kg, 14 d). P38MAPK: P38 mitogen-activated protein kinase; Tie2: angiopoietin receptor 2; Ang1: angiopoietin 1; Ang2: angiopoietin 2. [a]$P < 0.01$ *vs* S; [b]$P < 0.01$ *vs* M; [c]$P < 0.01$ *vs* NLXT.

significantly. Relative to the NLXT group, the five indexes for HXTL and YQ groups remarkably decreased, whereas the neurological deficit score significantly increased. Although the expression of relevant components of the VEGFA/VEGFR2 pathway after cerebral ischemia was different, they showed the same trend as CD31. In contrast, the p38 MAPK level significantly increased after cerebral ischemia but decreased after the intervention of Chinese medicine, especially in the NLXT group. Those showed that the trend of p38 MAPK was opposite to that of CD31, which is consistent with that found in the literature. The experimental results showed that compared with simple YQ herbs and HXTL herbs, YQHXTL herbs could significantly improve the neurological deficits in model rats, enhance posterior circulation ischemia, promote vascular regeneration, and increase cerebral blood flow.

Astragalus polysaccharide, the active ingredient of Huangqi (*Radix Astragali Mongolici*), can promote VEGF expression in rats through the covalent binding of cross-linking agent and polypeptide chain in collagen to promote angiogenesis at the injury site.[30] Studies have shown that Chinese medicines for promoting blood circulation and removing blood stasis can regulate the angiogenesis factors such as VEGF and basic fibroblast growth factor, can increase the vascular density, promote the establishment of collateral circulation in the acute phase of cerebral infarction, and increase blood supply to the penumbra of cerebral infarction.[31] Ligustrazine can inhibit the angiogenesis of human umbilical vein endothelial cells induced by oxidative density lipoprotein through the VEGF pathway.[32] Salvianolone IIA, the extract of Danshen (*Radix Salviae Miltiorrhizae*), can promote angiogenesis by upregulating VEGF expression which may be related to the up-regulation of HIF-1 α expression.[33] Danhong injection, extraction of Danshen (*Radix Salviae Miltiorrhizae*) and Honghua (*Flos Carthami*) can effectively improve the vascular endothelial function of patients with acute cerebral infarction.[34] Tianma (*Rhizoma Gastrodiae)* can promote neuronal regeneration and vascular regeneration by upregulating the expression of VEGF and VEGFR2.[35] The extract of Wugong (*Scolopendra*) could reduce the content and biological activity of plasma v WF and TPO in rats with focal cerebral reperfusion, improve endothelial cell injury and platelet function, effectively inhibit platelet adhesion and aggregation, and prevent thrombosis. Thus, it can reduce damage caused by cerebral ischemia reperfusion.[36]

NLXT is composed of *Qi*-tonifying herbs and blood-activating stasis-resolving collateral-dredging herbs. Huangqi (*Radix Astragali Mongolici*) is effective for tonifying *Qi* and blood, Danshen (*Radix Salviae Miltiorrhizae*) and Honghua (*Flos Carthami*) effectively promote blood circulation to remove blood stasis. Sanqi (*Radix Notoginseng*) effectively removes blood stasis and stops bleeding, and Tianma (*Rhizoma Gastrodiae)* and Wugong (*Scolopendra*) are effective for dredging meridians and collaterals. The experiment found that the YQHXTL, YQ, and HXTL herbs could promote angiogenesis in brain tissue of rats with MCAO/R syndrome of QDBS at different degrees. The effect was more significant in the NLXT group but weaker in the YQ and the HXTL groups. In TCM, Jun, Chen, Zuo, and Shi emphasized compatibility among herbs. The combination of different herbs can improve the curative effect of the original herbs and reduce the toxic and side effects of each other. For example, Wugong (*Scolopendra*) has low toxicity and better dredging meridians and collaterals when combined with other herbs. It is indicated that the synergy between different herbs can boost the curative effect of the whole prescription in promoting angiogenesis in rats with MCAO/R QDBS syndrome at the cellular level.

Based on the comprehensive research results, the specific mechanism of the different traditional Chinese herbs on vascular regeneration should be studied further. We used microvessel count to visualize angiogenesis. The main shortcoming of this experimental design is that the changes in mRNA expression of Ang1 and Ang2 could not directly reflect the changes in protein levels, which will be explored in our future *in-vitro* experiments.

5. SUPPORTING INFORMATION

Supporting data to this article can be found online at http://journaltcm.com.

6. REFERENCES

1. Putaala J. Ischemic stroke in young adults. Continuum (Minneap Minn) 2020; 26: 386-414.
2. Davis SM, Donnan GA. 4.5 hours: the new time window for tissue

plasminogen activator in stroke. Stroke 2009; 40: 2266-7.
3. Liang H, Xiao J, Zhou Z, et al. Hypoxia induces miR-153 through the IRE1α-XBP1 pathway to fine tune the HIF1α/VEGFA axis in breast cancer angiogenesis. Oncogene 2018; 37: 1961-975.
4. Zhao J, Du P, Cui P, et al. LncRNA PVT1 promotes angiogenesis *via* activating the STAT3/VEGFA axis in gastric cancer. Oncogene 2018; 37: 4094-109.
5. Hong S, Chen S, Wang X, et al. ATAD2 silencing decreases VEGFA secretion through targeting has-miR-520a to inhibit angiogenesis in colorectal cancer. Biochem Cell Biol 2018; 96: 761-68.
6. Claesson-Welsh L, Welsh M. VEGFA and tumor angiogenesis. J Intern Med 2013; 273: 114-27.
7. Sung JF, Fan X, Dhal S, et al. Decreased circulating soluble Tie2 levels in preeclampsia may result from inhibition of vascular endothelial growth factor (VEGF) signaling. J Clin Endocrinol Metab 2011; 96: E1148-52.
8. Muller WA. Leukocyte-endothelial-cell interactions in leukocyte transmigration and the inflammatory response. Trends Immunol 2003; 24: 327-34.
9. Cheung K, Ma L, Wang G, et al. CD31 signals confer immune privilege to the vascular endothelium. Proc Natl Acad Sci USA 2015; 112: E5815-24.
10. Zheng Y, Han Z, Zhao H, Luo Y. MAPK: a key player in the development and progression of stroke. CNS Neurol Disord Drug Targets 2020; 19: 248-56.
11. Liu B, Liu YJ. Carvedilol promotes retinal ganglion cell survival following optic nerve injury *via* ASK1-p38 MAPK Pathway. CNS Neurol Disord Drug Targets 2019; 18: 695-704.
12. He L, Shi X, Seto SW, et al. Using 3D-UPLC-DAD and a new method-verification by adding mixture standard compounds to determine the fingerprint and eight active components of Naoluoxintong decoction. J Pharm Biomed Anal 2019; 169: 60-9.
13. Bu L, Dai O, Zhou F, et al. Traditional Chinese Medicine formulas, extracts, and compounds promote angiogenesis. Biomed Pharmacother 2020; 132: 110855.
14. Xu SY. Pharmacological experimental methodology. Beijing: People's Medical Publishing House 1982: 535.
15. Tan H, Yin T, Deng Y, He L, Li F, Wang Y. Mechanisms of Yiqihuoxue herb Naoluoxintong promotes cerebral vascular regeneration in rats with cerebral ischemia syndrome of *Qi* deficiency accompanied by blood stasis. Xi Bao Yu Fen Zi Mian Yi Xue Za Zhi 2020; 36: 712-8.
16. Longa EZ, Weinstein PR, Carlson S, Cummins R. Reversible middle cerebral artery occlusion without craniectomy in rats. Stroke 1989; 20: 84-91.
17. Weidner N. Intratumor microvessel density as a prognostic factor in cancer. Am J Pathol 1995; 147: 9-19.
18. Ma C, Wang X, Xu T, et al. Qingkailing injection ameliorates cerebral ischemia-reperfusion injury and modulates the AMPK/NLRP3 inflammasome signalling pathway. BMC Complement Altern Med 2019; 19: 320.
19. Beck H, Plate KH. Angiogenesis after cerebral ischemia. Acta Neuropathol 2009; 117: 481-96.
20. Beck H, Acker T, Wiessner C, Allegrini PR, Plate KH. Expression of angiopoietin-1, angiopoietin-2, and tie receptors after middle cerebral artery occlusion in the rat. Am J Pathol 2000; 157: 1473-83.
21. Soker S, Miao HQ, Nomi M, Takashima S, Klagsbrun M. VEGF165 mediates formation of complexes containing VEGFR-2 and neuropilin-1 that enhance VEGF165-receptor binding. J Cell Biochem 2002; 85: 357-68.
22. Marti HH, Risau W. Systemic hypoxia changes the organ-specific distribution of vascular endothelial growth factor and its receptors. Proc Natl Acad Sci USA 1998; 95: 15809-14.
23. Monacci WT, Merrill MJ, Oldfield EH. Expression of vascular permeability factor/vascular endothelial growth factor in normal rat tissues. Am J Physiol 1993; 264: C995-1002.
24. Zhao Y, Fu B, Chen P, et al. Activated mesangial cells induce glomerular endothelial cells proliferation in rat anti-Thy-1 nephritis through VEGFA/VEGFR2 and Angpt2/Tie2 pathway. Cell Prolif 2021; 54: e13055.
25. Liang N, Li Y, Chung HY. Two natural eudesmane-type sesquiterpenes from Laggera alata inhibit angiogenesis and suppress breast cancer cell migration through VEGF- and Angiopoietin 2-mediated signaling pathways. Int J Oncol 2017; 51: 213-22.
26. Feng YH, Li LF, Zhang Q, et al. Microtubule associated protein 4 (MAP4) phosphorylation reduces cardiac microvascular density through NLRP3-related pyroptosis. Cell Death Discov 2021; 7: 213.
27. Piera-Velazquez S, Jimenez SA. Endothelial to mesenchymal transition: role in physiology and in the pathogenesis of human diseases. Physiol Rev 2019; 99: 1281-324.
28. Figueiredo CC, Pereira NB, Pereira LX, et al. Double immunofluorescence labeling for CD31 and CD105 as a marker for polyether polyurethane-induced angiogenesis in mice. Histol Histopathol 2019; 34: 257-64.
29. Wang Y, Zhang L, Pan YJ, et al. Investigation of invigorating *Qi* and activating blood circulation prescriptions in treating *Qi* deficiency and blood stasis syndrome of ischemic stroke patients: study protocol for a randomized controlled trial. Front Pharmacol 2020; 11: 892.
30. Yao C, Li A, Gao W, Pallua N, Steffens G. Improving the angiogenic potential of collagen matrices by covalent incorporation of Astragalus polysaccharides. Int J Burns Trauma 2011; 1: 17-26.
31. Yang BR, Cheung KK, Zhou X, et al. Amelioration of acute myocardial infarction by saponins from flower buds of Panax Notoginseng *via* pro-angiogenesis and anti-apoptosis. J Ethnopharmacol 2016; 181: 50-8.
32. Yuan R, Shi W, Xin Q, et al. Tetramethylpyrazine and paeoniflorin inhibit oxidized LDL-induced angiogenesis in human umbilical vein endothelial cells *via* VEGF and Notch pathways. Evid Based Complement Alternat Med 2018; 2018: 3082507.
33. Xu W, Yang J, Wu LM. Cardioprotective effects of tanshinone IIA on myocardial ischemia injury in rats. Pharmazie 2009; 64: 332-336.
34. Hu Z, Wang H, Fan G, et al. Danhong injection mobilizes endothelial progenitor cells to repair vascular endothelium injury *via* upregulating the expression of Akt, eNOS and MMP-9. Phytomedicine 2019; 61: 152850.
35. Liu M, Zhao L, Han L, et al. Discovery and identification of proangiogenic chemical markers from Gastrodiae Rhizoma based on zebrafish model and metabolomics approach. Phytochem Anal 2020; 31: 835-45.
36. Wang LN, He L, Cheng H, et al. Effects of centipede extraction on vWF and TPO expression in blood plasm after focal cerebral ischemia-reperfusion injury in rats. Zhong Guo Shi Yan Fang Ji Xue Za Zhi 2012; 18: 192-5.